ELSEVIER

PII: S0032-3861(96)00947-0

Polymer Vol. 38 No. 15, pp. 3957–3965, 1997

0032-3861/97/$17.00 + 0.00

The effect of the moulding conditions on the semicrystalline structure of polypropylene

A. Minardi, M. Boudeulle and E. Duval*
LPCML, URA 442 CNRS, Université Claude Bernard Lyon I, 43 boulevard du 11 Novembre 1918, 69622 Villeurbanne Cedex, France

and S. Etienne
LMPSM, URA 155 CNRS, Ecole des Mines de Nancy, Parc de Saurupt, 54042 Nancy Cedex, France
(Received 27 February 1996; revised 15 July 1996)

The semicrystalline structure of isotactic polypropylene (iPP) moulded by oscillating melt–flow (rheomoulding) has been studied using low-frequency Raman scattering (coupled with optical interference reflection microscopy and wide-angle X-ray scattering). It was compared to the structure of typically moulded iPP. We observed that only the relatively narrow central zone of the bar has a spherulitic organization in the rheomoulded specimen, while the external layers on each side have a perfectly oriented crystalline structure. The crystal structure, the orientation, the size of the crystallites and the effect of annealing were determined. © 1997 Elsevier Science Ltd.

(Keywords: poly(propylene); moulding; crystallinity)

INTRODUCTION

The complex crystalline structure and the commercial importance of isotactic polypropylene (iPP) have stimulated intensive research work. The studies devoted to the crystal structures and crystal morphologies and the different preparation conditions favouring one or other of the polymorphs of iPP are summarized by Brückner *et al.*[1]. The two most common crystalline phases, extensively studied by Natta *et al.*[2], show monoclinic (α) and hexagonal (β) packing, respectively. Both crystalline structures can coexist in a given specimen, but with each spherulite consisting of one single phase. It has been shown that the α spherulites are characterized by the presence of transversal crystallites which grow by homo-epitaxy on the radial lamellae[3,4]. This branching is often refered to as 'cross-hatching'. Obviously the mechanical properties of semicrystalline iPP are strongly dependent on the semicrystalline microstructure and on the crystalline–amorphous linking. Aboulfaraj *et al.*[5] studied the plastic deformation of iPP under uniaxial tension and showed the difference of behaviour between β spherulites and branched α spherulites.

The semicrystalline structure depends on the rheological conditions occurring during the processing. In the work which is presented in this paper, the semicrystalline microstructure of specimens, moulded by oscillating the melt–flow[6], was compared to that of specimens moulded under the usual conditions. The textural and structural organization have been studied using optical interference reflection microscopy, and wide-angle X-ray scattering (WAXS) (diffractometry and flat plane camera). Particular attention has been devoted to the investigation of the molecular arrangement, using low-frequency Raman scattering (LFRS). By LFRS, one observes the longitudinal acoustic modes (LAMs), localized along the helical chains of the crystallites. The frequency of the LAMs informs us on the length of the regions of helical chains in ordered packing.

EXPERIMENTAL

Samples

The iPP was a homopolymer of Hunstman chemical (grade 5520). The melt flow index was 5, according to ASTM, and the density 0.903 g cm^{-3} at 23°C. The melting temperature (T_m) was determined by d.s.c.: T_m = 168°C. The specimens were moulded by injection–compression. Two different series of plates were compared: some were moulded without vibrating the melt flow, while others were moulded by vibrating the melt flow by means of additional lateral pistons[6]. The specimens obtained by melt vibrating are called 'rheomoulded'[6]. Each plate was moulded in a dog-bone shape. The samples were cut from the central part as indicated in *Figure 1*.

Optical interference reflection microscopy

For the observation of the spherulitic structure with a Reichert Polyvar microscope the faces to be observed were etched by immersion for 18 h, at room temperature, in the solution recommended by Olley

* To whom correspondence should be addressed

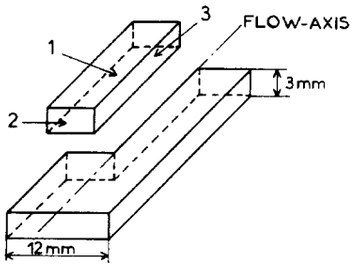

Figure 1 Cutting of the sample in the central part of the moulded or rheomoulded specimen. The observed faces are marked by a number

and Basset[7] (1.3 wt% potassium permanganate, 32.9 wt% concentrated H_3PO_4 and 65.8 wt% concentrated H_2SO_4) and finally were gold coated by sputtering.

Low-frequency Raman scattering

To observe the Raman scattering from longitudinal acoustic modes the surface of the sample was illuminated by means of an argon or krypton laser delivering an incident light beam of wavelength 514.5 or 647.1 nm, respectively. The incidence angle was close to $\pi/2$. The light scattered approximately at $\pi/2$ relatively to the incident laser beam was analysed with a 4 m focal length quintuple monochromator and detected with a photon-counting system. The linear polarization of the laser beam could be adjusted.

Wide-angle X-ray scattering

X-ray diffractometer scans were recorded with a Siemens D500 diffractometer (λ CuKα = 1.540 Å, graphite back monochromator, step scan procedure, 0.02° ($2\Theta\,s^{-1}$). Transmission X-ray patterns using a flat camera (λ MoKα = 0.709 Å) were obtained in order to confirm the interpretations drawn from diffractometry. Crystallinity ratio and peak fitting, assuming a split Pearson-7 shape, were computed with the corresponding programs from the Siemens DIFFRAC-AT software package.

RESULTS

Optical interference reflection microscopy

Faces 2 and 3 (see *Figure 1*) were observed. A spherulitic structure was observed for the whole thickness of the moulded specimen. The size of the observed spherulites, formed mostly of α crystallites, was between 10 and 50 μm in diameter. The observations with the rheomoulded specimen were totally different (*Figure 2*). A spherulitic structure was observed in the central zone of the cross-section. The thickness of this spherulitic zone is about 500 μm, with the specimen having a thickness of 3 mm. The size of the spherulites is about 50 μm in the central zone and decreases from the centre to the edges (*Figure 1*). It is possible to see, in *Figure 2*, a tilting-like structure, oriented along the specimen axis, at the frontier of the spherulitic zone (*Figure 2*). No heterogeneous crystalline structure was observed outside of the

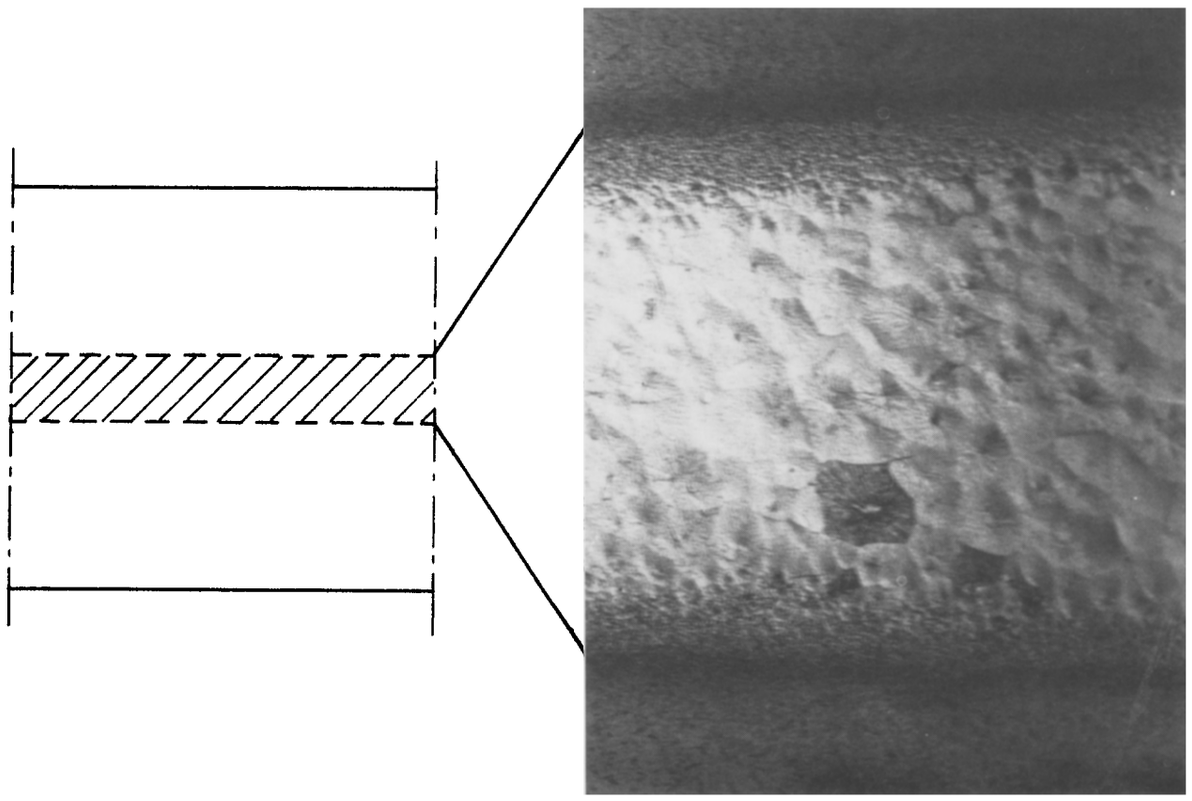

Figure 2 Face 2 of the sample and the corresponding image of the spherulitic central zone of rheomoulded specimens obtained with the optical interference reflection microscope (×160). The layers in each side of the central zone appear homogeneous. The darkest spherulite corresponds to the β phase

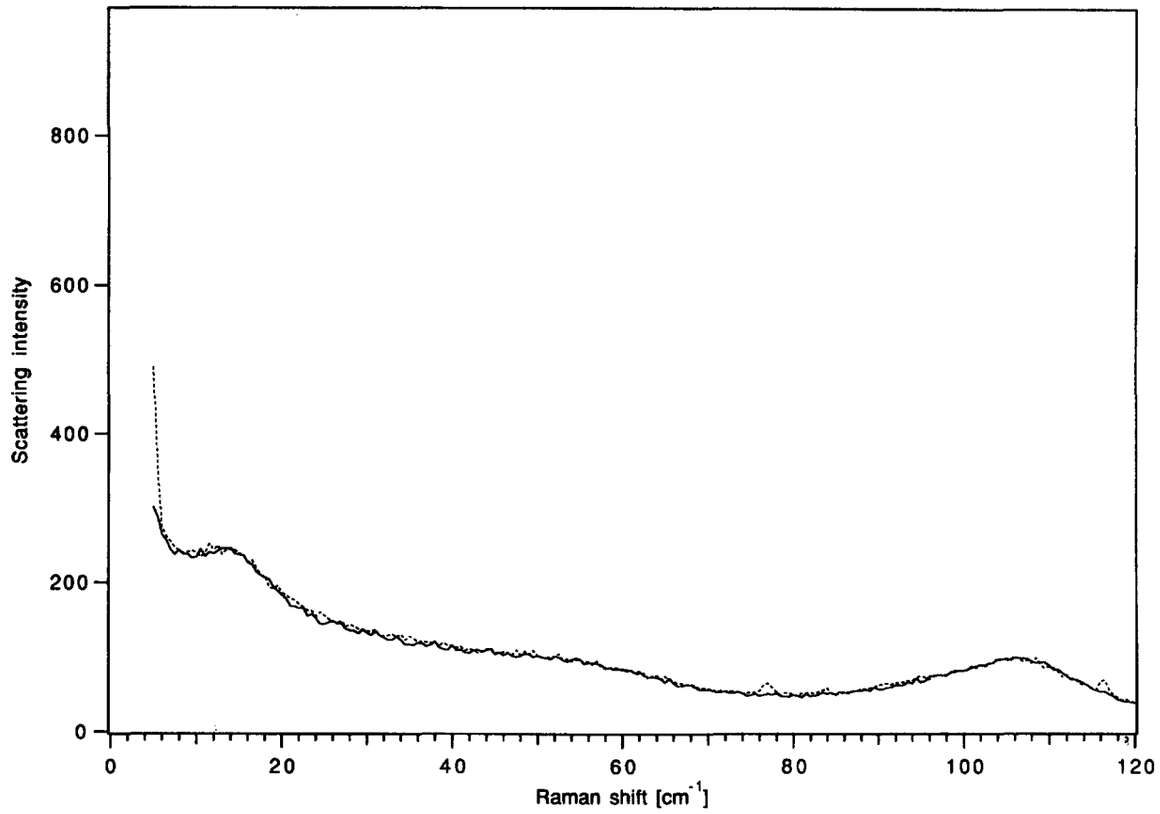

Figure 3 LFRS spectra of the moulded iPP sample. VV spectrum, full line; HH spectrum, dashed line. The laser beam is incident on face 1

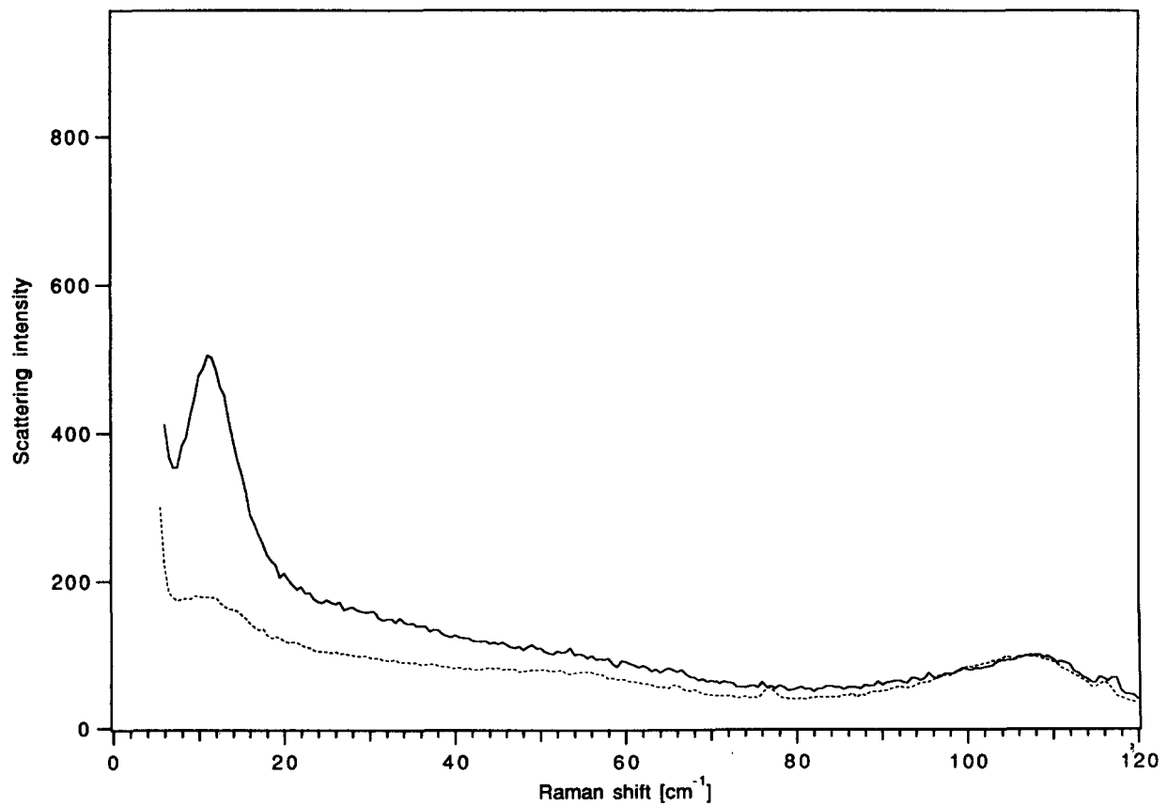

Figure 4 LFRS spectra of the rheomoulded iPP sample. VV spectrum, full line; HH spectrum, dashed line. The laser beam is incident on face 1

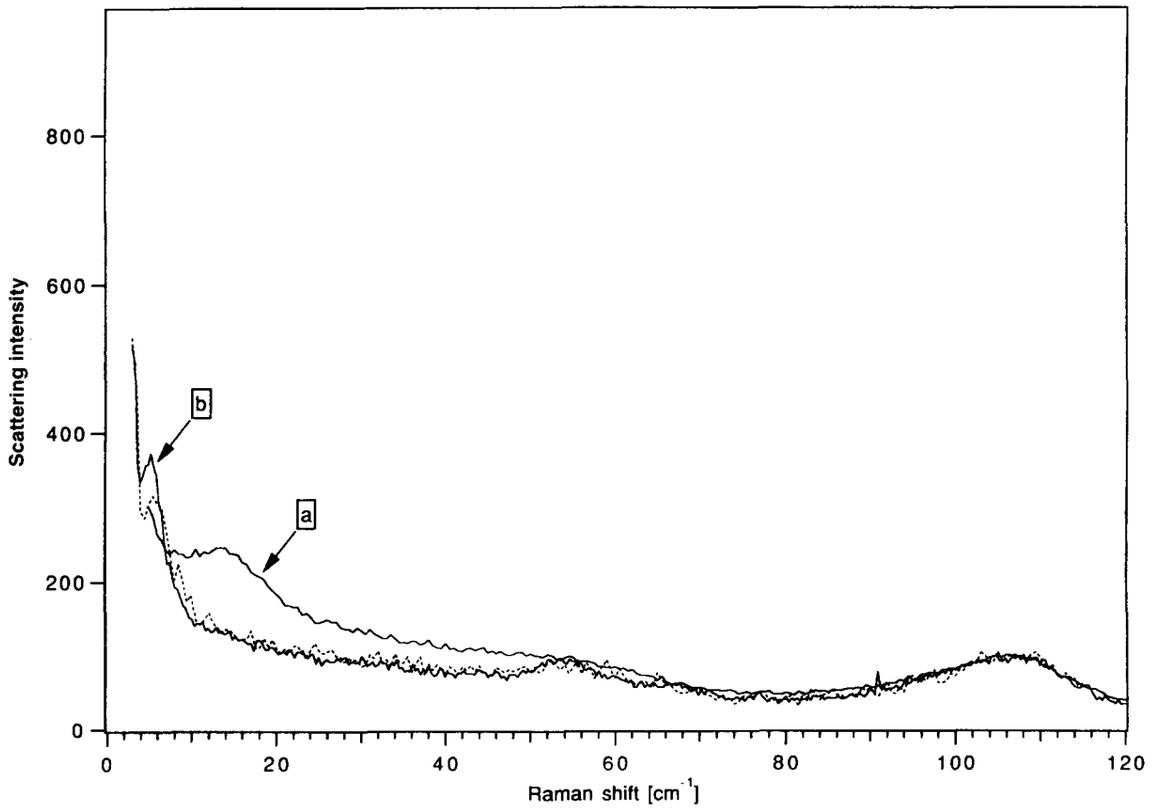

Figure 5 LFRS spectra of the moulded iPP sample. (a) VV spectrum before annealing. (b) VV spectrum after annealing for 20 min at 170°C Corresponding HH spectrum (dashed line)

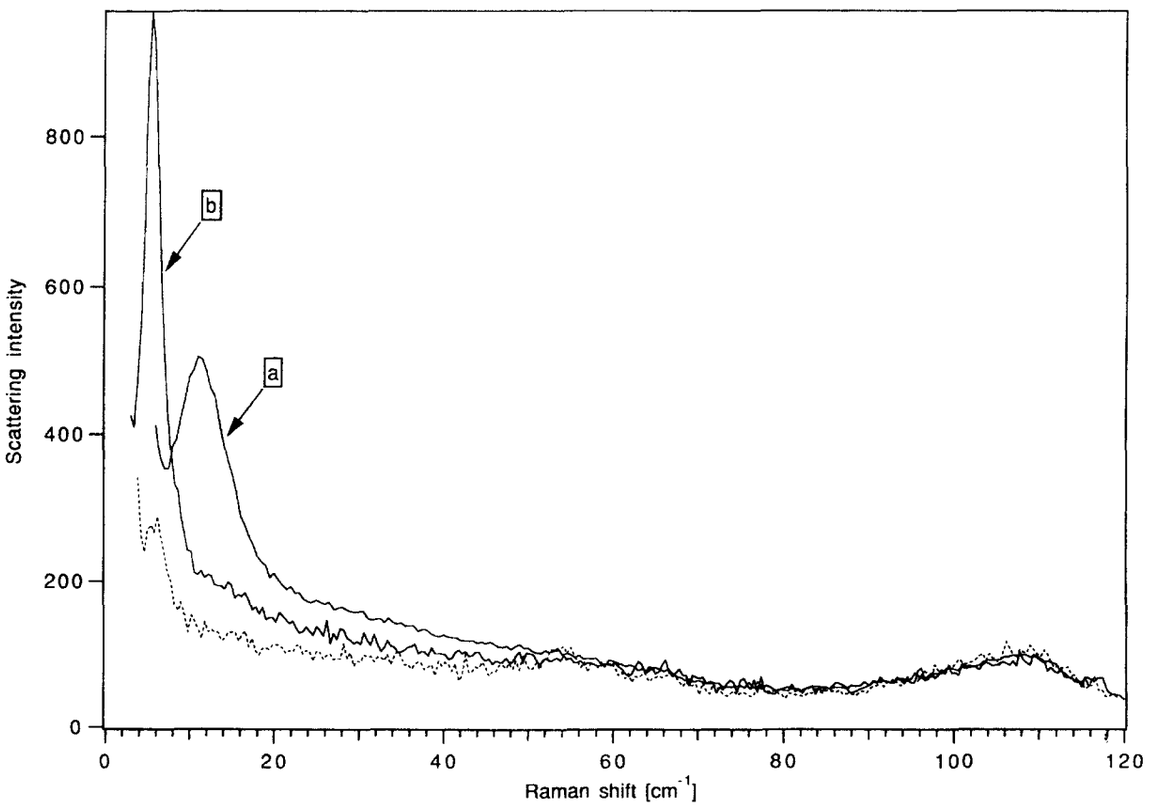

Figure 6 LFRS spectra of rheomoulded iPP sample. (Same key as for Fig. 3)

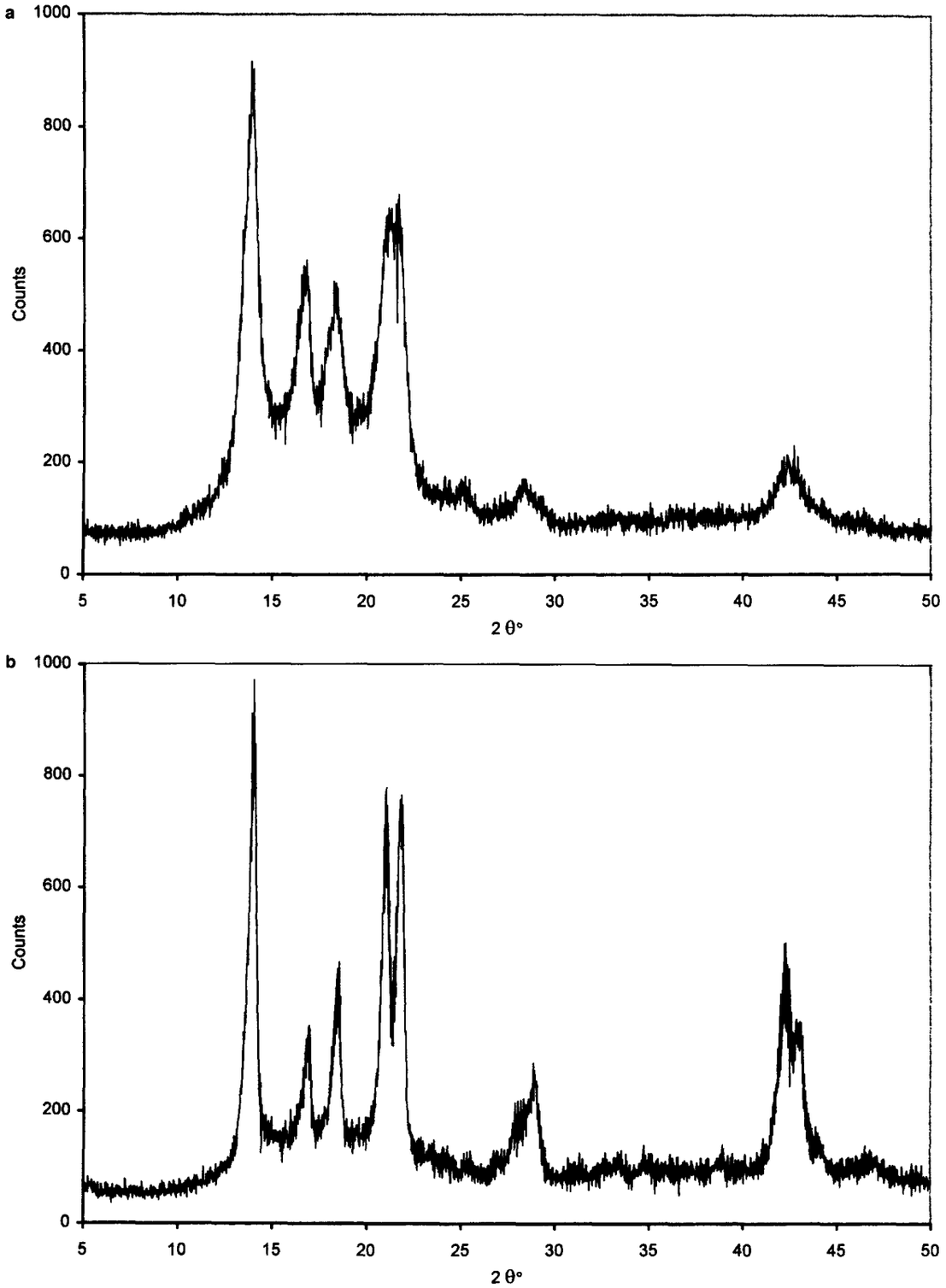

Figure 7 WAXS of moulded iPP. (a) Raw material. (b) After annealing at 170°C for 20 min

central spherulitic zone. Scanning electron microscopy confirmed these observations.

Low-frequency Raman scattering

The LFRS Stokes spectra, in the 5–120 cm^{-1} spectral range, are shown in *Figures 3* and *4* for the moulded and rheomoulded specimens, respectively. The laser beam was incident on face 1 of the sample (see *Figure 1*). The VV spectra obtained with the laser and scattering polarizations parallel to the flow axis were compared with the HH spectra for polarizations perpendicular to the axis. The main feature in these spectra is the presence of a band at 12–14 cm^{-1}, which will be assigned, as shown below, to the LAMs, and consequently is called the LAM peak. The intensity of this peak is identical in the VV and HH spectra for the moulded iPP; however, it is much stronger in the VV than in HH spectra ($I_{VV}/I_{HH} > 5$) for the rheomoulded iPP. Furthermore, it

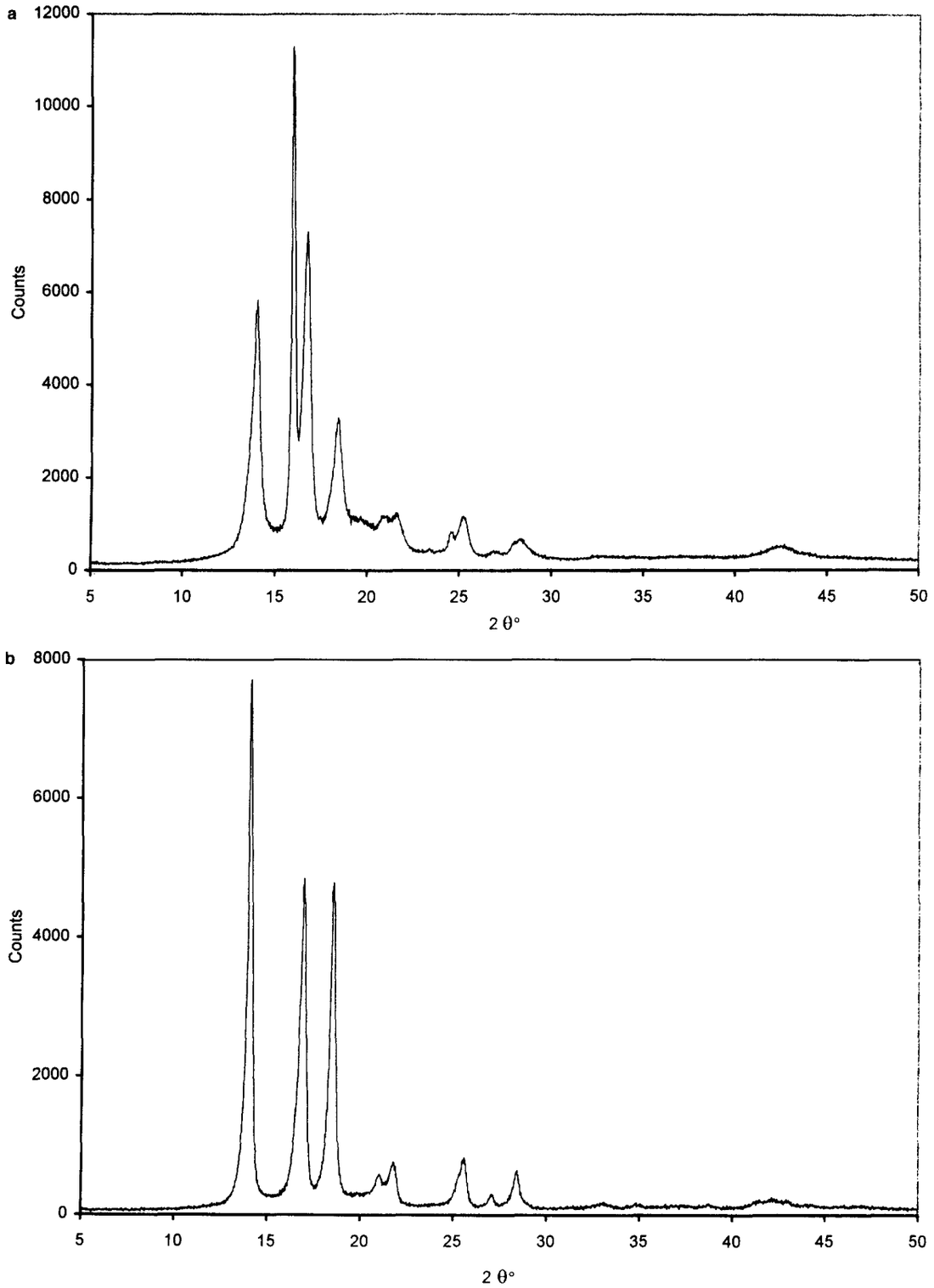

Figure 8 WAXS of rheomoulded iPP. (a) Raw materials. (b) After annealing at 170°C for 20 min

was observed that the LAM peak is weaker in crossed polarizations, with V polarization for the laser beam and H for the scattered light ($I_{VH}/I_{VV} \approx 0.3$).

The LFRS was also observed, the laser beam being incident on face 3. When the laser illuminated the middle of the face, therefore principally the spherulitic zone, the intensity of the LAM peak at 13 cm^{-1} was not much higher in VV polarization than in HH polarization.

Moulded and rheomoulded samples were annealed in air for 20 min at different temperatures between 60 and 170°C. A shift of the LAM peak towards the Rayleigh line was observed in the spectra taken at room temperature (*Figures 5* and *6*). It was a maximum after heating at 170°C, i.e. a temperature slightly higher than the melting temperature of the α phase. For the rheomoulded iPP the effect of annealing was

spectacular, as shown in *Figure 6*: the LAM peak shifted, after heating at 170°C for 20 min, from 11.5 cm^{-1} to 5.7 cm^{-1}, and became narrower. A similar shift was observed for the moulded iPP. After heating, and with the laser beam incident on face 1 of the specimen, the LAM peak was more strongly polarized than before for the rheomoulded iPP (*Figure 6*) ($I_{VV}/I_{HH} \approx 10$). Such a polarization effect was not observed for the moulded iPP (*Figure 5*).

Wide-angle X-ray scattering

In *Figures 7a* and *8a* are shown the diffractometer scans exhibited by the raw moulded and rheomoulded specimens, respectively. The RX beam was incident on face 1 of the sample (*Figure 1*).The sharpness of the diffraction peaks for the rheomoulded sample is remarkable (*Figure 8a*). The peaks of the monoclinic α phase[2] are observed (*Figure 8a*) at $2\theta = 14°$, 16.8, 18.5°,..., corresponding respectively to the ($hk1$) planes (110), (040), (130),.... An extra very narrow peak is observed at $2\theta = 15.8°$, which is peculiar to the hexagonal β phase[8]. Such a narrowness of the peaks indicates a high degree of perfection of the crystallites in the rheomoulded specimen with large coherent domain in the directions orthogonal to the chain axis. For the moulded specimen (*Figure 7a*) the peaks are much broader. However, the intensity of the reflection from the α phase at $2\theta = 21°.3$, which corresponds[2] to the (111) planes, is much stronger for the moulded specimen than for the rheomoulded one.

The diffraction profiles of both specimens after annealing for 20 min in air are shown in *Figures 7b* and *8b*. The crystallinity ratio reaches about 75% for the rheomoulded sample, compared with about 50% for the two samples prior to annealing. The peaks are narrower, and for the rheomoulded sample one observes a pattern of highly ordered α crystallites (the reflection at 15°.8 coming from the β phase has vanished). It should be noticed that the line profiles for the ($hk0$) reflections are much less asymmetric after heating, confirming the increasing crystal order. The intensity of the (111) reflection remains very weak for the rheomoulded sample, when an opposite behaviour is observed for the same reflection for the heated moulded sample.

Transmission diffraction patterns recorded with the X-ray beam orthogonal to face 1 are shown in *Figures 9a* and *9b*. The rheomoulded material exhibits a typical fibre pattern superimposed on a faint Debye–Scherrer one. The fibre-like axis, parallel to the chain axis, lies along the length of the bar, thus indicating a high degree of molecular orientation for the major part of the sample. In comparison, the Debye–Scherrer rings exhibited by the other sample are coherent, with a random spherulitic organization as described above.

DISCUSSION

Optical interference reflection microscopy

From *Figure 2*, the effect of rheomoulding is spectacular: only the central zone (relative to the specimen thickness of 3 mm), with a thickness of 500 μm, is spherulitic. The other part of the specimen is homogeneous on the microscopic scale. In contrast, the moulded specimen is wholly spherulitic. Due to the viscosity, the oscillation of the melt flow induces a vibrating shear stress, parallel to the mould walls, which decreases from the walls to the core. The effect of this shear stress is to orientate the polymer chains, thus favouring the growth of well-ordered crystallites, and then to prevent the misorientation of the crystallites and the formation of spherulites. This is the reason why the sample appears homogeneous on the microscopic scale, but not in the 500 μm central zone.

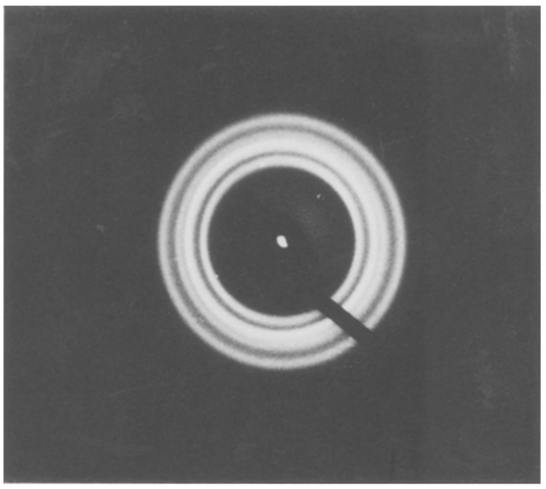

(a)

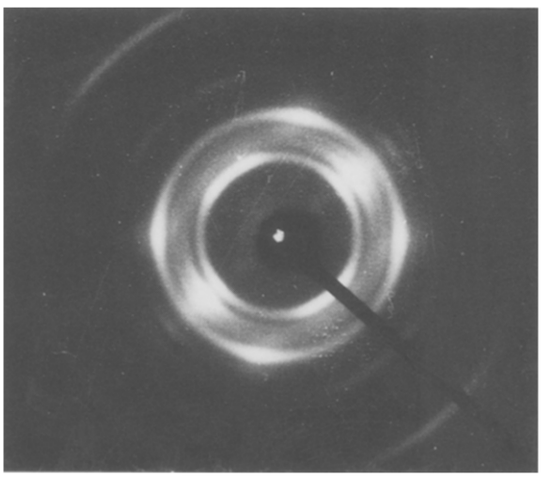

(b)

Figure 9 Transmission diffraction patterns recorded with the X-ray beam orthogonal to face 1. The axis of the plate is parallel to the beam stop. (a) Moulded sample. (b) Rheomoulded sample

Low-frequency Raman scattering

In the LFRS spectra of unannealed moulded and rheomoulded specimens (*Figures 3* and *4*), in addition to the LAM peak one observes a vibration band at 106 cm^{-1}, which is assigned to the CH_2–$CHCH_3$ polymer backbone torsion[9,10], and a broad band which spreads from the Rayleigh line up to 80 cm^{-1}. This broad band is due to the Raman scattering from acoustic modes, which are localized in the iPP nanocrystallites or which are non-propagating because of the disorder, as observed in amorphous polymers[11]. It is likely that, close to the Rayleigh line and the LAM peak, there is a contribution of quasi-elastic scattering due to relaxation motions in the amorphous phase at a temperature higher than $T_g(= -20°C)$.

Table 1 Position of LAM peak and helix length

	Moulded iPP		Rheomoulded iPP	
	Non-heated	Heated for 20 min at 170°C	Non-heated	Heated for 20 min at 170°C
LAM peak (cm^{-1})	13.8	5.5	11.5	5.5
ℓ (nm)	8.8	22.1	10.6	22.1

Table 2 FWHM of the diffraction peak at $\theta = 14°$

Sample	*FWHM* (°)
Raw moulded	0.866
Annealed moulded	0.630
Rheomoulded	0.5246
	0.207[a]
Annealed rheomoulded	0.273

α phase: *FWHM* for (110) reflection
[a] β phase: *FWHM* for (300) reflection

Because the LAM peak is associated with crystallite morphology, we are particularly interested in it. The Raman scattering by the low-frequency longitudinal acoustical vibrational modes propagating along the molecular chains in crystallites was first observed a long time ago in semicrystalline n-paraffins[12,13]. It was also observed for LAMs propagating along the axis of helical chains[14] and, in particular, in semi-crystalline iPP[15]. In a simple model of a continuous elastic rod, the fundamental frequency of the LAM is given by[13]

$$\nu = \frac{(E/\rho)^{1/2}}{2\ell} \tag{1}$$

where ℓ corresponds to the length of the molecular helix, E being the elastic Young modulus in the direction parallel to the chain screw axis and ρ the density of the iPP crystal. The corresponding Raman shift expressed in wave-numbers (cm^{-1}) is

$$\omega = \frac{(E/\rho)^{1/2}}{2\ell c} \tag{2}$$

where c is the velocity of light in free space. What we have called the LAM peak corresponds to the Raman scattering by the fundamental LAM. The LAM overtones are not visible in experimental Raman spectra (*Figures 3–6*). With $E = 50$ GPa[16] and $\rho = 936\,kg\,m^{-3}$ [17], from the positions of LAM peak and equation (2), we find the molecular helix lengths in crystallites, which are given in *Table 1*. Comparing our results with those obtained by Rabolt and Franconi[17], who give the long period determined by small-angle X-ray scattering assuming amorphous lamellae sandwiched between crystalline lamellae, we find that the thickness of the crystalline lamellae is two times larger than that of the amorphous domains and four times larger after heat treatment at 170°C.

As observed for the rheomoulded specimen (*Figure 6*), the full width at half-maximum (*FWHM*) is three times sharper after annealing, which means that the average size distribution of the crystallites in the thickness is about three times narrower after heat treatment.

The principal difference between rheomoulded and moulded samples is the polarization of the LAM peak, when the laser excites the vibrations not in the core zone but close to the specimen surface. In the rheomoulded sample, the LAM peak is much more intense for the polarizations of incident and scattered light parallel to the long axis of the specimen than for other polarization configurations. It means that the chains in crystallites are oriented along the long flow axis of the specimen and that the polarizability has a maximum for incident and scattered electric fields parallel to the long axis. No such polarization or orientation was observed for the moulded sample.

What is remarkable is that the polarization and orientation become even stronger after annealing at 170°C in the rheomoulded sample. Now it is well known that there is a growth of transversal crystallites by homo-epitaxy on the principal radial lamellae[3,4] upon heating, the angle between the principal lamellae and the transversal ones being 80°. Consequently the strong polarization indicates that no such branching or 'cross hatching' of the crystallites occurs through heating in the rheomoulded specimens. One reason for that would be the macromolecular chains also being oriented in the amorphous part by the rheomoulding processing.

Wide-angle X-ray scattering

Comparison of *Figures 7* and *8* shows that the diffraction peaks, from the surface layers of the sample, are much sharper for the rheomoulded specimen (in the non-spherulitic zones) than for the moulded one. As suggested by Vittoria[17], the size and degree of perfection of α crystallites can be evaluated from the *FWHM* of the peak at $2\theta = 14°$, which corresponds to the (110) reflection. The *FWHM* values are given for both specimens, before and after annealing at 170°C, in *Table 2*. The *FWHM* values are almost two times smaller for the rheomoulded samples that for the moulded ones and, as usual, both *FWHM* values decrease after annealing at 170°C (*Figures 7b* and *8b*), indicating that the packing order within the α crystallites increases. The average size of the coherent domains is larger in the rheomoulded specimen, along the [110]* direction, orthogonally to the oriented molecular chains, prior to and after the heat treatment. After annealing, the very low value of the FWHM, which indicates a domain size in the width of the crystallites two times larger than in the raw material, and the line profile symmetry, evidence of the uncommonly high degree of crystalline order of the α phase.

Another clear difference is that the intensity of the (111) and (003) reflections is very weak in the rheomoulded specimen compared to the moulded one (*Figures 7* and *8*). That is confirmation that the crystallites are oriented, with the [001] direction parallel to the flow axis in the rheomoulded specimen, outside the spherulitic central zone. Such an orientation does not exist in the moulded specimens.

In *Figure 8a*, the sharpness of the peak at 15.8° (*FWHM* = 0.21°, compared to the intrinsic experimental widening of 0.135° which has been determined for the apparatus), which corresponds to the (300) reflection of the β phase[7] is noticeable. Another reflection of the hexagonal phase at 21°, which corresponds to (301) planes[7], is not visible. This confirms that the β crystallites, like the α ones, have, outside the spherulitic central zone, a tremendous crystal order and are oriented with the [001] direction parallel to the flow axis in the

sample. The crystallization of the β phase induced by shear flow had already been observed by Dragaun *et al.*[18]. After heating at 170°C, the β crystallites are transformed into α crystallites, because of the higher melting temperature of the latter.

CONCLUSION

The complementary methods which were used in this research show clearly the effect of the rheomoulding processing on the iPP microstructure. The central zone of the sample in the cross-section, which is six times thinner than the thickness of the specimen, exhibits a spherulitic structure. The structure of the crystallites in the spherulites is mostly monoclinic (α). The oscillating melt flow induces shear stresses which prevent the formation of spherulites in the thicker layers on each side of the spherulitic central zone. In these external layers, the observed α and β crystallites exhibit molecular chains oriented along the flow axis, the length of regularly oriented polymer chain fractions being approximately equal to 10 nm. The structural order of the crystallites is higher in the oriented external layers than in the spherulitic central zone. In contrast, the structure is completely spherulitic in the simply moulded iPP material, which presents a lower crystallinity ratio.

After annealing at 170°C, the β crystallites are transformed into α crystallites. The orientation is preserved and even enhanced, like the structural order, in the external layers of the rheomoulded samples. The length of the oriented polymer chains increases from about 10 to 22 nm, the size distribution becoming much narrower, while the width of the crystallites doubles. No branching or 'cross hatching' was observed in the oriented α crystallites after heating. In parallel, the observed evolution seems compatible only with a high degree of chain orientation in the 'amorphous' phase, which probably shows some kind of nematic organization induced by the shearing during the processing. It is expected that the mechanical properties of the isotactic polypropylene are strongly modified by rheomoulding.

ACKNOWLEDGEMENTS

The authors are very grateful to R. F. Callahan, from Thermold, for providing the specimens, and to J. P. Ibar, from Eknet Research, for discussions about this research.

REFERENCES

1. Brückner, S., Meille, S. V., Petraccone, V. and Pirozzi, B., *Progr. Polym. Sci.*, 1991, **16**, 361.
2. Natta, G. and Corradini, P., *Nuovo Cim. Suppl.*, 1960, **15**, 40.
3. Norton, D. R. and Keller, A., *Polymer*, 1985, **26**, 704.
4. Albrecht, T. and Strobl, G., *Macromolecules*, 1995, **28**, 5267.
5. Aboulfaraj, M., G'Sell, C., Ulrich, B., and Dahoun, A., *Polymer*, 1995, **36**, 731.
6. Ibar, J. P., *Modern Plastics*, 1995, **25**, 85.
7. Olley, R. H. and Basset, D. C., *Polymer*, 1989, **30**, 399.
8. Gomez, M. A., Tanaka, H. and Tonelli, A. E., *Polymer*, 1987, **28**, 2227.
9. Miyazawa, T., Fukushima, K. and Ideguchi, Y., *J. Polym. Sci. (B)*, 1963, **1**, 385.
10. Goldstein, M., Steeley, M. E., Willis, H. A. and Zichy, V. J. I., *Polymer*, 1973, **14**, 530.
11. Achibat, T., Boukenter, A., Duval, E., Lorentz, G. and Etienne, S., *J. Chem. Phys.*, 1991, **95**, 2949.
12. Mizuchima, S. and Shimanouchi, T., *J. Am. Chem. Soc.*, 1949, **71**, 1320.
13. Schaufele, R. F. and Shimanouchi, T., *J. Chem. Phys.*, 1967, **47**, 3605.
14. Hartley, A., Leung, Y. K., Booth, C. and Stepherd, I. W., *Polymer*, 1976, **17**, 355.
15. Hsu, S. L., Krimm, S., Krause, S. and Yeh, G. S. Y., *J. Polym. Sci., Polym. Lett. Ed.*, 1976, **14**, 195.
16. Lacks, D. J. and Rutledge, G., *Macromolecules*, 1995, **28**, 115.
17. Rabolt, J. F. and Franconi, B., *J. Polym. Sci., Polym. Lett. Ed.*, 1977, **15**, 121.
18. Dragaun, H., Hubeny, H. and Muschik, H., *J. Polym. Sci., Polym. Phys.*, 1977, **15**, 1779.